SPE Brazil Flow Assurance Technology Congress
Rio de Janeiro, Brazil, November 15 – 18 2022

Visualization of wax deposit formation and growth by using MRI on a laboratory wax flow loop

Imane Yalaoui[1,3,4], Loïc Barré[1], Thibaud Chevalier[1], Myriam Darbouret[2*], Pierre Levitz[3] and Thierry Palermo[4]
[1]IFP Energies nouvelles, Rueil-Malmaison, France
[2]IFP Energies nouvelles, Solaize, France, *myriam.darbouret@ifpen.fr
[3]PHENIX, Sorbonne University, 4 place Jussieu, 75005 Paris, France
[4]TotalEnergies, Research and Development Flow Assurance, CSTJF Pau, France

Abstract
An innovative set-up was designed to study wax deposit formation along time despite the opacity of the media without disturbing the flow. It consists in a laboratory wax flow loop, integrated into an MRI (Magnetic Resonance Imaging) device. This paper shows the results obtained using a synthetic oil under laminar flow. The MRI was used to acquire density and velocity maps at different times. Results evidenced that, depending on the imposed temperatures, it was possible to obtain a static layer at the wall by two different mechanisms: either by a progressive wax crystals enrichment near the cold wall or by rapid gelation of the oil at the wall. Moreover, this technique allowed an observation of the structure of a wax deposit and of its heterogeneities. This deposit is potentially composed of two layers: a consolidated layer rich in crystals at the wall and an unconsolidated layer less rich in crystals with liquid in circulation inside. This method which is compliant with real crude oil characterization offers a promising way to obtain useful inputs for the modeling such as, deposit thickness, growth kinetics and the wax crystals concentration.

Keywords
Wax deposit, kinetics, Magnetic Resonance Imaging.

Introduction
Numerous studies have been made for years in efforts to understand wax deposition mechanisms and predict the kinetics of the wax deposit growth. This information is needed to design the operation scheme and the pigging frequency that will be required in order to limit the wax deposit thickness to maximum value (2 to 4 mm depending on operators). Despite these efforts, there is still a need to improve the accuracy of predictive tools in order to reduce safety margin and allow new operational strategies that will enable to reduce the production cost for waxy crude oil.
Different predictive tools exist. They all consider wax deposition mechanisms based on wax diffusion to the cold wall and can offer the possibility to consider kinetics effects or aging effect. Most of the time, user-defined inputs are necessary but not so easy to define such as wax concentration in the deposit, diffusion coefficient, viscosity of the crude oil… [1].

Experimental wax deposition studies mainly rely on set-ups (flow loops for example) which often provide macroscopic measurements such temperatures, flow rates, pressure drop. A wax deposit thickness can be derived from the pressure drop measurement based on the hypothesis that the presence of the deposit causes a reduction in diameter but the impact of temperature and rheological behaviour of the crude oil are more complex to take into account. Even if some efforts have been made to provide visualization with synthetic oil [2], due to the opacity of the crude oils, no direct observation can be made under flow condition. Wax deposits observations require to stop the flow, dry the line and open the pipe. The wax deposit can then be sampled and further analyzed.
Moreover, most of the time, very low wall temperatures are imposed to promote wax deposition in experimental set-ups. The drawback of this kind of protocol is that near the wall, the low temperature can change drastically the rheological behavior of the oil as well as the wax deposition mechanism. In such a case, the scaling up of experimental results is then questionable if the experimental conditions are not representative of conditions that can be encountered on the field.

The motivation of this study was to develop an innovative set-up which enables to gain insights of the wax deposition mechanisms by following along time the wax deposit building-up.

Methodology

This section describes the materials, experimental set-up and experimental methodologies used for this study.

Synthetic oil preparation and characterization

A synthetic oil (oil A) was prepared using a dearomatized aliphatic oil (Hydroseal G250H (C15-C20), number C.A.S 8002-74-2, crystallization temperature ≥ 65 °C) density 0.812 g/cm3 at 20 °C and 5 % weight of wax (commercial wax purchased from Prolabo, melting point 52-54 °C).

The WAT and the weight fraction of wax crystals C_{wax} (wt.%) of the oil were obtained with a differential scanning calorimeter (DSC). The WAT of this synthetic oil was measured at 36 °C. The detailed procedures have been described in [3].

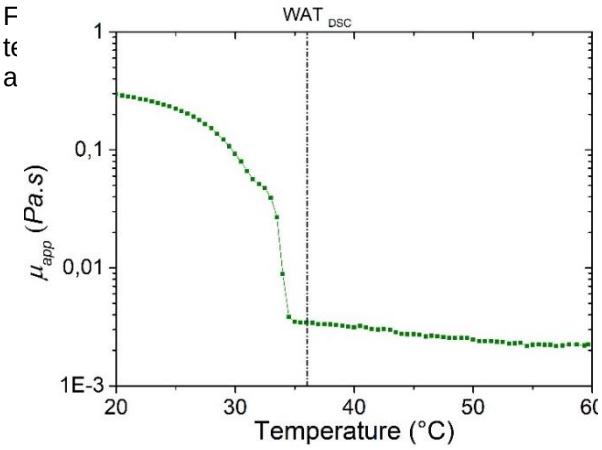

Figure 1. Viscosity of oil A (shear rate $\dot{\gamma}$ = 15 s^{-1}).

Experimental flow-loop

The designed flow loop aims at reproducing and studying the issues related to the production and transport of waxy crude oils in pipeline. The particularity of this loop is that it has been designed to be integrated in the 20 MHz MRI from Oxford Instrument. A diagram of the flow loop is given in Fig. (2). The flow loop is instrumented by a differential pressure sensor, temperature sensors, and a mass flowmeter.

The total volume of the loop is about 1 L (+ 2L in the oil tank). The measurement section of the loop consists in a vertical pipe-in-pipe glass tube. The inner pipe diameter is 10 mm in diameter and 1.50 m long, through which the hot paraffinic fluid circulates. A 26 mm diameter outer tube allows the co-current circulation of a heat transfer fluid used for controlling the temperature of the inner wall pipe. Temperature can be controlled in range [20 °C - 80 °C]. The temperature in the jacketed cell, where the wax deposit is formed, is measured using PT100 probes placed at the inlet and outlet of the pipe with an accuracy of 0.5 °C. The flow rates range from 1 L/h to10 L/h, corresponding to shear rates from 3 s^{-1} to 30 s^{-1}. MRI operates at a temperature of 30 °C. For this study, a synthetic oil with a high WAT (Wax Appearance Temperature) (36 °C) was selected so that it can be easily handled in the laboratory conditions without having to over-cool the oil to induce the formation of the wax deposit. Longitudinal localization is ensured by a displacement of the jacketed cell relative to the MRI magnet. This displacement is carried out by a manual arm that keeps the cell vertical inside the MRI device.

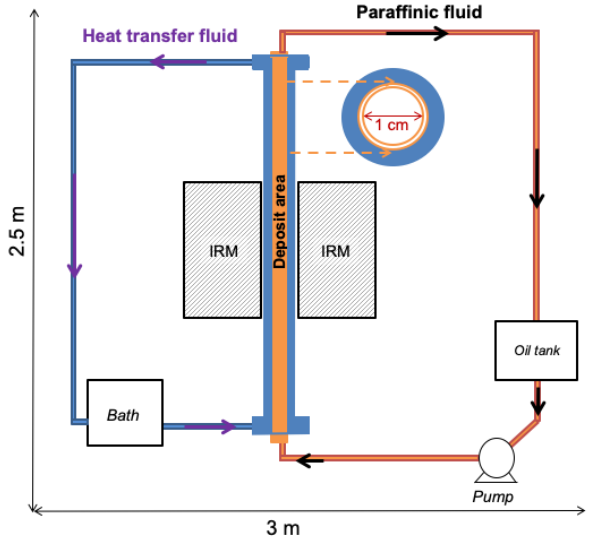

Figure 2. Schematic of the flow-loop.

The aim of the tests performed on the flow loop is to form a wax deposit at the wall of the inner pipe and to study its characteristics and its structuration along time.

The bulk fluid was set above the WAT so that paraffins do not crystallize in the circulating fluid and no intensity loss is observed at the center of the pipe during MRI measurements.

The parameter of interest was the subcooling, defined as the difference between the WAT of the paraffinic fluid and the temperature of the heat transfer fluid.

Table 1 sums up the experimental conditions.

Table 1. Test matrix.

Test	Flow rate (L/h)	T_{cold} (°C)	T_{hot} (°C)
Test 1	5	(WAT-7°C)	(WAT+7°C)
Test 2	5	(WAT-2°C)	(WAT+2°C)

For the chosen test conditions the Reynolds number is 48. The measurements are made on a section located at L = 75 cm from the inlet of the pipe. At this location, the hydrodynamic flow regime and the thermal regime are well developed.

Determination of the wax crystals content in the deposit

The objective is to quantify the local wax crystal content from the density maps assuming that the intensity loss can be associated with the presence of wax crystals [1].

From density maps, we can determine the size of the regions where a loss of intensity is detected, from which we can deduce the quantity of wax crystals, knowing the volume of a wax crystal.

Acquisition protocol

During the test, we acquire a density map, a flow velocity map and then a reference velocity map at zero speed. For the reference velocity maps, the flow is stopped for about 5 min and then restarted. The reference map is required to have the velocity in the tube. The MRI measurements were performed in the center of the pipe (75 cm) on a 4 mm thick slice.

Results and Discussion

High subcooling test results

Test 1 was performed with a very low wall temperature T_{cold} =WAT - 7°C in order to promote wax deposition at the wall.

Figure 3 shows the velocity profiles obtained along the time. For this test, the velocity profiles is modified very rapidly and then do not evolved along time. A large (~2,6mm) zero-velocity region appeared very rapidly at the wall, whereas a Poiseuille flow is observed in a reduce diameter pipe, with an increase of the maximum velocity (~16 cm/s) due to flow rate conservation. No wax crystals enrichment was detected from density measurement in the static zone. The kinetics of the phenomenon and the absence of wax crystals enrichment evidences a gelation effect: the fluid stops locally due to its rheological behavior in the low temperature zone: the shear stress imposed by the flow is not sufficient to flow the oil at this low temperature [5], [6]. This static layer is not representative of wax deposits that can be observed in a real field where temperature difference between the bulk and the wall will be smaller. Nevertheless, this test enligthed a source of errors linked to the experimental procedures with very low wall temperature.

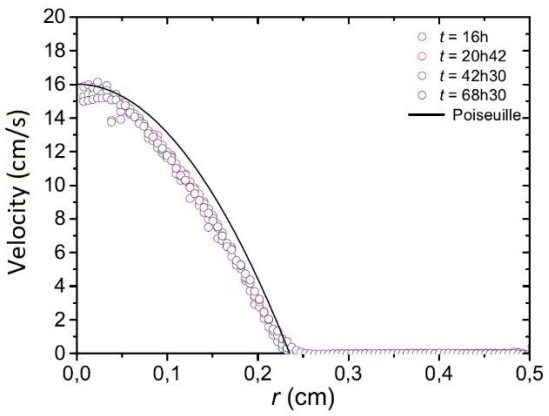

Figure 3: Velocity profiles measured during Test 1 (averaged on 2 π) (empty circles) and Poiseuille profile (full line). (*r=0* is the center of the pipe)

Low subcooling test results

Figure 4 shows velocity profiles measured along Test 2. At *t = 0h*, the velocity profile follows a classical Poiseuille profile, corresponding to a laminar flow of a Newtonian fluid. At *t = 24h10* and *116h*, the temperature of the fluid close to the wall decreases and its viscosity increases. The velocity profile is modified by the high-viscosity zone into a bell-shaped velocity profile. In a first approach, the velocity profile may still be described using a Poiseuille velocity profile but with a smaller pipe diameter. Consequently, due to flow rate conservation, the maximum velocity increases at the center of the pipe: *t =24h10* (≈ 4.9 cm/s) than at *t = 0h* (≈ 3.7 cm/s).

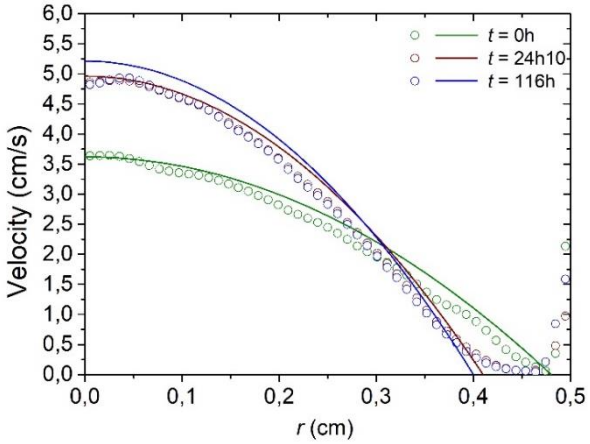

Figure 4. Velocity profiles measured during Test 2 (averaged on 2 π) (empty circles) and Poiseuille profile (full lines). (*r=0* is the center of the pipe)

Figure 5 presents density maps obtained along time for Test 2. Different ranges of intensity loss, directly corresponding to different crystals contents, have been defined.

The images show that the amount of crystals are, on the average, greater near the wall than at the center of the flow. In addition, images confirm that the loss of intensity becomes increasingly significant over time at certain points in the deposit, reflecting the enrichment of the deposit at these locations. These observations show that the deposit is enriched over time in a localized manner from the center of the flow towards the wall (richer in crystals), probably by molecular diffusion.

These density maps evidence that the wax deposit obtained is not homogeneous neither radially, nor on the circumference of the pipe. The observation of a heterogeneous deposit is consistent with the observations of Morozov et al. [4] who were able to observe and monitor the formation of the wax precipitation process in a cold finger cell by MRI.
The wax deposit enrichment along time is also evidenced. Both the wax deposit average diameter and its wax crystals concentration increase.

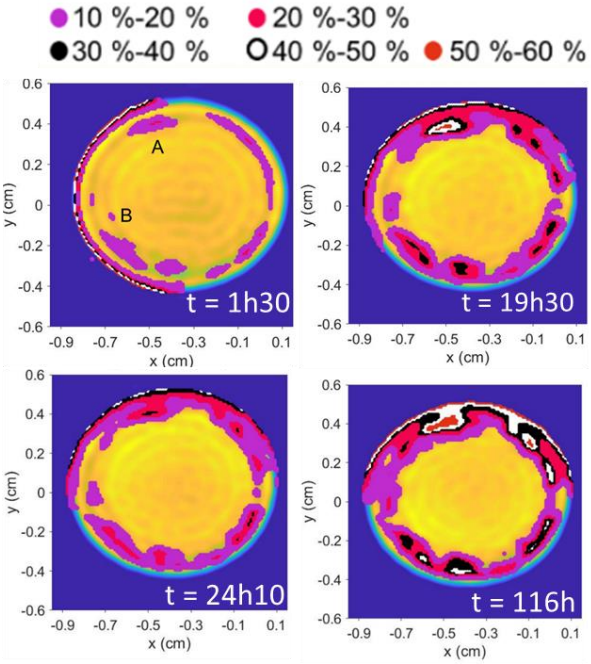

Figure 5. Density maps with the different intensity loss ranges calculated over time ((a) *t = 1h30*, (b) *t = 19h30*, (c) *t = 24h10* and (d) *t = 116h*).

For a complete understanding of the nature of the flow taking place at a specific time of the experiments, it is worth coupling the velocity and wax crystals concentration provided by the MRI technique. This is done on Figure 6 for *t = 116h*. This figure provides both the radial velocity profile and an equivalent volume of crystallized *n*-paraffins (both profiles are averaged on 2- π).

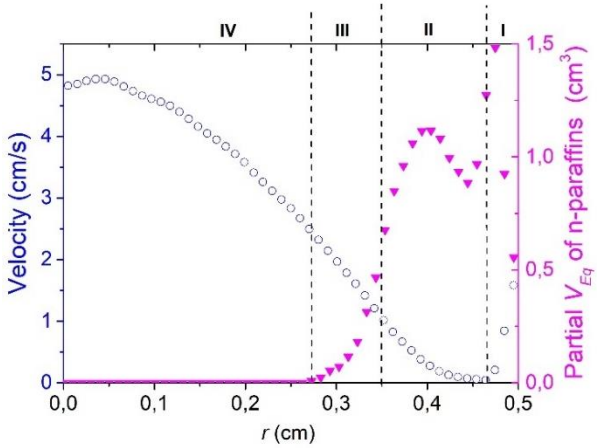

Figure 6. Comparison between the radial velocity profile (empty symbol) obtained at *t=116h* and the radial profile of the equivalent volume of crystallized n-paraffins (solid symbols).

From the comparison between these profiles, several zones can be identified: zone IV is a high velocity zone (0 cm < r < 0.27 cm) free of wax crystals, zone III (0.27 cm < r < 0.35 cm) is a zone containing a small amount of wax crystals but which is not sufficient to impact the flow, zone II is a high viscosity zone, in which the velocity profile shows an inflexion point (0.4 cm < r < 0.47 cm) and finally zone I is a static (no velocity) layer at the cold wall, poorly defined due to the vicinity of the wall.

Conclusions

This study showed that MRI is a promising technique to study of wax deposition under flow conditions, providing both wax crystals concentration and velocity profiles along wax deposition process. Real-time monitoring of wax crystals concentration profiles and velocity profiles allowed a good description of the mechanisms of formation, growth and aging of a wax deposit. A gelation effect was evidenced for a high subcooling. For low subcooling, evolutions of the velocity and density profiles, showed the formation of a heterogeneous deposit, mostly composed of liquid with slow kinetics of growth and enrichment. It is potentially composed of two layers: a consolidated layer rich in crystals at the wall and an unconsolidated layer less rich in crystals with liquid in circulation inside (Fig. (6)).

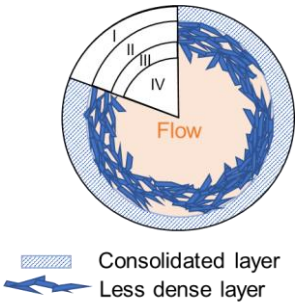

Figure 6. Schematic structure of the wax deposit in the pipe for low subcooling.

Acknowledgments

The authors would like to thank TotalEnergies for the financial support and for permission to publish these results.

Responsibility Notice

The authors are the only responsible for the paper content.

References

[1] Van der Geest, Melchuna A, Bizarre L., Bannwart A., Guersoni V., *Fuel* 293 (2021) 120358
[2] Azevedo : *Energy Fuels 2020*, 34, 12182−12203
[3] Yalaoui, I.; Chevalier, T.; Levitz, P.; Darbouret, M.; Palermo, T.; Vinay, G.; Barré, L. *Energy Fuels 2020*, 34 (10), 12429–12439.
[4] Morozov E.V.; Falaleev O.V., Martyanov O.N., *Energy & Fuels, 30 (2016)*, 9003-9013.
[5] Benallal, A.; Maurel, P.; Agassant, J. F. , Darbouret, M.; Avril, G.; Peuriere, E. SPE Annual Technical Conference and Exhibition, 2008
[6] Zheng S., Saidoun M., Palermo T., Mateen K., Fogler S., *Energy Fuels 2017,* 31, 5011−5023